

**Geological and Petrophysical Information in Geophysical
Inversion Problems**

by

Daniel Bild-Enkin

BSc Honours, The University of Toronto, 2012

A THESIS SUBMITTED IN PARTIAL FULFILLMENT
OF THE REQUIREMENTS FOR THE DEGREE OF

Masters of Science

in

THE FACULTY OF GRADUATE AND POSTDOCTORAL
STUDIES
(Geophysics)

The University of British Columbia
(Vancouver)

August 2016

© Daniel Bild-Enkin, 2016

Abstract

Preface

Table of Contents

| | |
|---|-------------|
| Abstract | ii |
| Preface | iii |
| Table of Contents | iv |
| List of Tables | vii |
| List of Figures | viii |
| Glossary | x |
| Acknowledgments | xi |
| 1 Introduction | 1 |
| 1.1 Research Motivation | 1 |
| 1.2 Regularized Inversion | 3 |
| 1.3 Literature Review | 5 |
| 1.4 Thesis Organization | 8 |
| 2 Tools for Integrating Geological and Petrophysical Information into Regularization | 10 |
| 2.1 Including Sample Information (Bore Hole and Surface Sample) in Inversion Regularization | 10 |
| 2.1.1 Importing Bore Hole Data | 11 |
| 2.1.2 Visualizing Bore Hole Data | 15 |

| | | |
|----------|---|-----------|
| 2.1.3 | Converting Lithology Information into Petrophysical Information | 16 |
| 2.1.4 | Discretizing Bore Hole Data | 16 |
| 2.1.5 | Editing Bore Hole Data | 17 |
| 2.1.6 | Making Constraint | 17 |
| 2.1.7 | Surface Sample | 18 |
| 2.2 | Including Geological Maps in Inversion Regularization | 19 |
| 2.2.1 | Preprocessing images | 19 |
| 2.2.2 | Loading Images into GIFtools | 20 |
| 2.2.3 | Creating a Pixel Map Legend | 21 |
| 2.2.4 | Making a Geology Model from Map | 23 |
| 2.2.5 | Making Constraints for an Inversion | 26 |
| 2.2.6 | Inputing Fault information from Geological Maps | 27 |
| 2.3 | Clustering to Create Pseudo-geologic Constraints | 31 |
| 2.3.1 | Clustering Algorithms | 31 |
| 2.3.2 | Clustering In GIFtools and Model Builder | 32 |
| 2.3.3 | Creation of Constraints | 33 |
| 2.4 | Voxel-Parametric Inversion to Provide Physical Property Values for Geological Models | 33 |
| 2.4.1 | Formulation of Voxel-Parametric inversion problem | 35 |
| 2.5 | Conclusion | 36 |
| 3 | Case Study #2 TKC | 37 |
| 3.1 | Overview of Deposits | 38 |
| 3.2 | Discussion of the Geophysical Data Given | 38 |
| 3.3 | What Information is Available | 38 |
| 3.4 | Synthetic Model | 38 |
| 3.5 | Blind Inversion of the Synthetic Model | 38 |
| 3.6 | Determination of Magnetization Dirrection | 38 |
| 3.7 | Creation of Constraints and Types of Data | 38 |
| 3.7.1 | α coefficients | 38 |
| 3.7.2 | Reference Models | 38 |
| 3.7.3 | Weighting matrices | 38 |

| | | |
|----------|---------------------------------------|-----------|
| 3.7.4 | Bounds | 38 |
| | Bibliography | 39 |
| A | Supporting Materials | 41 |

List of Tables

| | | |
|-----------|--|----|
| Table 2.1 | An example collar file from TKC bore holes | 11 |
| Table 2.2 | An example survey file from TKC bore holes (same holes as Table 2.1 | 12 |
| Table 2.3 | An example survey file from TKC bore holes (same holes as Table 2.1 | 13 |

List of Figures

| | | |
|-------------|--|----|
| Figure 2.1 | The first Graphical User Interface (GUI) for importing bore hole data | 14 |
| Figure 2.2 | The second GUI for importing bore hole data | 15 |
| Figure 2.3 | Visualization of TKC lithology bore hole data | 16 |
| Figure 2.4 | Visualization of El Poma susceptibility bore hole data | 16 |
| Figure 2.5 | GUI to allow the discretization of bore hole data to a given mesh | 18 |
| Figure 2.6 | The El Poma map with fault lines (blue lines with barbs) included | 20 |
| Figure 2.7 | The El Poma map with extra information removed and geological units made a single colour | 20 |
| Figure 2.8 | GUI for importing plan view image | 21 |
| Figure 2.9 | GUI for importing cross section image | 22 |
| Figure 2.10 | Example of magnetics data being viewed with a map overlaid | 22 |
| Figure 2.11 | Example of a geology model created from a map with the map overlaid | 24 |
| Figure 2.12 | Example of a 2D mesh with the map overlaid | 25 |
| Figure 2.13 | Example of a 2D geology model created from a cross section map with the map overlaid | 25 |
| Figure 2.14 | GUI for adding a 2D model to a 3D model | 26 |
| Figure 2.15 | Example of a 2D geology inserted into a 3D model with the map overlaid | 26 |
| Figure 2.16 | Example of a geological definition as displayed in the GIFtools GUI | 27 |
| Figure 2.17 | Example of a typical combine model dialog for a reference model | 28 |

| | | |
|-------------|---|----|
| Figure 2.18 | Example of a reference model created from a geological map . | 29 |
| Figure 2.19 | The GUI for the creation of fault weights | 29 |
| Figure 2.20 | An example of fault weights that can be created with GIFtools | 30 |
| Figure 2.21 | Point cloud of the geological interfaces for TKC bore hole data | 33 |
| Figure 2.22 | A geological model created from the data shown in Figure 2.21 | 34 |

Glossary

This glossary uses the handy `acroynym` package to automatically maintain the glossary. It uses the package's `printonlyused` option to include only those acronyms explicitly referenced in the \LaTeX source.

| | |
|------------|--------------------------------|
| MOF | Model Objective Function |
| GIF | Geophysical Inversion Facility |
| GUI | Graphical User Interface |
| FCM | Fuzzy C-Means |

Acknowledgments

Thank those people who helped you.

Don't forget your parents or loved ones.

You may wish to acknowledge your funding sources.

Chapter 1

Introduction

1.1 Research Motivation

In mineral exploration there are many forms of information that can be used to determine the location of an economic deposit. These can be divided broadly into geological and geophysical data. Geological data refers to the study of the rocks in a region through surface samples, bore holes, and an understanding of how rock units interrelate under the surface. Geophysical data refers to recovered measurements of some field that is related to the physical properties of the rocks that will aid in the understanding of the deposit. For exploration to be as effective as possible, we need to find ways of integrating the geological and geophysical information that produce exploration vectors to the target. One of the major tools in using geophysical data to create geologically significant interpretations is inversion.

The overarching goal of geophysical inversion is to recover distributions of physical properties in the ground to aid in mineral exploration. To be useful to this end the spacial distribution of the physical property (the geophysical model) needs to both fit the geophysical data and match existing geological interpretations.

Since geophysical inversions are by their nature non-unique (because of data uncertainty and there typically being many more model parameters than data), *a priori* information needs to be added to provide a model that matches the geology

of a deposit. Much work has been done to create a mathematical framework to allow the inclusion of geological and petrophysical information into geophysical inversions (for example Li and Oldenburg (1996)). However, an area where more work must be done is the creation of tools to take the petrophysical and geological data in the forms that are generally provided and create usable constraints that can be applied to inversions.

The research in this thesis will attempt to do exactly that: provide new tools in an integrated framework that will allow the incorporation of non-trivial *a priori* information into geophysical inversions. The inclusion of *a priori* information in inversions is not novel. Many researchers, especially at the Geophysical Inversion Facility (GIF), before me have used the mathematical framework to add geological and petrophysical information to inversions (for example Lelievre 2009,Phillips 2001, Farquharson et al. 2008).

In addition, in Williams (2008) develops a software package to create constraints for inversions from a wide array of data types. What is lacking in the previous research is the link between the creation of inversion constraints with the processing of data and the running of inversions. By integrating the tools I create in this thesis into the framework of GIFtools and Model Builder I attempt to provide this link.

GIFtools and Model Builder are a suite of tools who's origins date back to Williams (2008), but which have been sufficiently updated that they deserve further treatment now. The goal now, as in Williams (2008), is to create a set of Graphical User Interface (GUI) tools that make the running of GIF inversion codes simple and easy. Model Builder, first described and implemented in Williams (2008), is, similarly, a set of GUI tools to make constraints for GIF inversion codes.

By intergrating these two sets of tools into one, I make the incorporation of *a priori* information into inversions much more expedient, thus encouraging greater uptake by industry. In total GIFtools and Model Builder allow users do quality control on data, create constraints, and run inversions within the same software framework. The interface by which *a priori* information can be incorporated has been much updated from Williams (2008), and tools to incorporate new forms of data into inversions have been added.

1.2 Regularized Inversion

In the general case, geophysical inversion involves the solving of a system that is defined by some forward operator that maps from a given model to predicted data,

$$\mathbf{d} = \mathbb{F}[\mathbf{m}], \quad (1.1)$$

where $\mathbf{d} \in \mathbb{R}^N$ is the geophysical data (and N is the number of data collected), $\mathbf{m} \in \mathbb{R}^M$ is a discretization of m which is the model that describes the distribution of some physical property (M is the number cells in the earth model), and \mathbb{F} is the forward operator that mediates between them. In the context of this thesis, \mathbf{d} is either magnetic or gravity data measured with a ground or aerial survey, \mathbf{m} is either a susceptibility or density model, and \mathbb{F} is the magnetic or gravitational forward operator which has the convenient property of being linear. Since we are interested in recovering the model \mathbf{m} , we are interested in finding the inverse of \mathbb{F} ,

$$\mathbf{m} = \mathbb{F}^{-1}\mathbf{d}. \quad (1.2)$$

Unfortunately the inversion of \mathbb{F} is far from trivial as the problem is ill-posed. Firstly since there are usually more model parameters than data ($M > N$) there are an infinite number of possible distributions of the physical property that will predict the observed data. Secondly the system is unstable, that is, a small amount of error in the measurements can lead to large changes in the recovered model. To recover a model despite these difficulties, the problem is regularized by adding *a priori* information in the form of a Model Objective Function (MOF) or regularization functional. Once the problem is regularized, it is solved by minimizing the objective function,

$$\phi(\mathbf{m}) = \phi_d + \beta \phi_m \quad (1.3)$$

where ϕ is the objective function, ϕ_d and ϕ_m are the data and model objective functions respectively, and β is a tradoff parameter that scales between them. ϕ_d is defined as a least squares (or L_2) formulation,

$$\phi_d = \|\mathbf{W}_d(\mathbb{F}[\mathbf{m}] - \mathbf{d}^{obs})\|^2 \quad (1.4)$$

$$\mathbf{d}^{obs} = \mathbb{F}[\mathbf{m}^{true}] + \mathbf{e} \quad (1.5)$$

where \mathbf{d}^{obs} is the observed data, that is the true data contaminated with noise \mathbf{e} , and \mathbf{W}_d is the data weighting matrix with the diagonal entries equal to the reciprocal of each datum's standard deviation,

$$\mathbf{W}_d = \begin{bmatrix} \frac{1}{\sigma_1} & 0 & \cdots & 0 \\ 0 & \frac{1}{\sigma_2} & 0 & \vdots \\ \vdots & \ddots & & 0 \\ 0 & \cdots & 0 & \frac{1}{\sigma_N} \end{bmatrix}, \quad (1.6)$$

where each σ_i is that datum's assigned standard deviation. Meanwhile ϕ_m is can take many forms. In Li and Oldenburg (1996) it is defined in the continuous formulation as,

$$\begin{aligned} \phi_m = & \alpha_s \|\mathbf{w}_s [(\mathbf{m} - \mathbf{m}_{ref})]\|^2 + \dots \\ & \alpha_x \|\mathbf{w}_x \mathbf{G}_x [(\mathbf{m} - \mathbf{m}_{ref})]\|^2 + \dots \\ & \alpha_y \|\mathbf{w}_y \mathbf{G}_y [(\mathbf{m} - \mathbf{m}_{ref})]\|^2 + \dots \\ & \alpha_z \|\mathbf{w}_z \mathbf{G}_z [(\mathbf{m} - \mathbf{m}_{ref})]\|^2. \end{aligned} \quad (1.7)$$

The first term in Equation 1.7 promotes smallness, that is the model must be close in value to the reference model \mathbf{m}_{ref} which is some first guess at the structure of the area being inverted. The next three terms promote smoothness by penalizing large derivatives in the model, determined by the discrete gradient operator \mathbf{G} in each direction. There are many parameters in ϕ_m that the geophysicist can use to fine-tune the recovered model. $\alpha_s, \alpha_x, \alpha_y$, and α_z , scale the contribution of smallness and smoothness in each spatial direction. α values can be used to broadly determine the length scales in each direction of a recovered model. The $\mathbf{w}_s, \mathbf{w}_x, \mathbf{w}_y, \mathbf{w}_z$ parameters allow finer control. They weight the model's smallness and smoothness variable across its extent allowing the user to specify certain regions as smoother than others or demanding that the recovered model more closely match the reference model in areas where the user is more certain of the reference model's validity.

In Equation 1.7 it is assumed the the norm of the regularization is L_2 .

$$\|\mathbf{v}\|_2 = \left(\sum_{i=1}^N v_i^2 \right)^{\frac{1}{2}} \quad (1.8)$$

this formulation can be generalized to a L_p norm that takes the form

$$\|\mathbf{v}\|_p = \left(\sum_{i=1}^N v_i^p \right)^{\frac{1}{p}} \quad (1.9)$$

where p is some positive number. Lower values of p promote more sparsity in the vector \mathbf{v}

The last term in Equation 1.3 is β which determines the degree to which the model fits the data or obeys the regularization. Its value is determined iteratively. Assuming that the error in \mathbf{d}^{obs} and Gaussian and independent with the standard deviations in \mathbf{W}_d , ϕ_d will be a random variable with a χ^2 distribution and an expected value of N , the number of data. Given this expected value, beta can be iteratively decreased until the misfit is sufficiently near N .

Now that I have given an overview of the structure of regularized inversion I will now discuss previous research on including geological and petrophysical information in inversion using regularization.

1.3 Literature Review

Firstly, there has been much research following the lines of Li and Oldenburg (1996) and Li and Oldenburg (1998). The methods used in these two papers are described above. The advantage of using least-squares methods for the regularization of inverse problems is that the objective function is convex, continuous, and differentiable, which greatly aids the implementation of the optimization. As mentioned above, reference models and weighting matrices allow for the incorporation of geological information, making smallness and smoothness more significant or less significant in different parts of the model. Li and Oldenburg (2003) extend the method by also implementing upper and lower bounds that can be specified for each model cell allowing the user to make hard constraints on the value of the model.

The above methods described in Li and Oldenburg (1996), Li and Oldenburg (1998), Li and Oldenburg (2003) recover smoothly varying models with broad distributions of the physical property. Sometimes the geological context indicates that the model should vary sharply and the anomalous body should be compact. In other words, either the model or its derivative should be sparse. There has been a great deal of research on using sparsity-promoting norms to achieve compact or sharply-varying models.

Instead of regularizing by smallness and smoothness, Last and Kubik (1983) regularize by compactness, essentially demanding that the anomaly be as small as possible while still fitting the data. They use an L_0 norm on the smallness component and do not use the smoothness constraints. Portniaguine and Zhdanov (1999) extend Last and Kubik (1983) by adding a minimum gradient support functional. The effect of this support functional is a L_0 norm on the smoothness terms instead of the smallness term as in Last and Kubik (1983).

Rudin et al. (1992) and Vogel and Oman (1998) propose total variation methods, in other words the use of L_1 norms to regularize, instead of L_2 norms as in Li and Oldenburg (1996) and Li and Oldenburg (1998). Since minimizing L_1 norms promotes sparsity, regularizing by them will have a comparable effect (blocky models with sharp boundaries) as the method used by Last and Kubik (1983) and Portniaguine and Zhdanov (1999). Total variation has been used more specifically in the context of geophysical inversion, such as with Guitton (2012).

Farquharson and Oldenburg (1998) also report ways of achieving sharp contrast by implementing non- L_2 norms such as Eklblom and Huber norms. Fournier (2015) implements a method of minimizing the general L_p (smallness) and L_q (smoothness) norms for any p and q (typically values between 0 and 2) allowing a user to specify the degree of compactness or blockiness of a recovered model in different spatial directions.

The formulation in Equation 1.7 allows a great deal of control of the way the model varies along the three cardinal directions. However, the geometry of a deposit does not always align with any of the cardinal directions and diagonal structures are preferred. Li and Oldenburg (2000) extend the method of Li and Oldenburg (1996) and Li and Oldenburg (1998) by rotating the model objective function to allow for linear features in the recovered model to be in a direction not in line

with the mesh grid. Lelièvre and Oldenburg (2009) generalize the methods in Li and Oldenburg (2000) to the 3D case.

Guillen and Menichetti (1984) extend the method in Last and Kubik (1983). Instead of minimizing the volume of a deposit, the authors minimize its moment of inertia. By specifying an axis of rotation to determine the moment of inertia, they put dip information into the regularization in addition to having the sharp contrasts and compact models as in Last and Kubik (1983). Barbosa and Silva (1994) and Barbosa and Silva (2006) extend the method even further allowing multiple axes of rotation. The second paper also describes a GUI to interactively test the fit of various axes of rotation.

Chasseriau and Chouteau (2003) create a very general method of biasing the inversion algorithm towards anomalies of almost any shape by weighting the smallness term with a covariance matrix of the model, i.e., a matrix with the covariance of each cell versus every other cell in the model. The covariance matrix can be generated from bore hole or surface sample data or from a synthetic initial model.

In addition to the deterministic inversions described above, much research has been done on stochastic inversion. Bosch et al. (2001) directly invert for lithologies. The authors forward model physical properties by a probabilistic relation of the physical property to the lithology. New lithology distributions are created using a pseudo-random walk. *A priori* information is included partially in the probabilistic model that links the lithology to the physical properties but also in the initial probability distribution of the lithology model. Guillen et al. (2008) implement the method described in Bosch et al. (2001) in 3D.

Attempts have also been made at combining stochastic and deterministic methods. One particularly successful line of inquiry are Fuzzy C-Means (FCM). Paasche et al. (2006) uses FCM clustering of recovered models to derive membership functions of model cells in several clusters. The clusters are then used with *a priori* porosity data to create a likely porosity of each cluster and a porosity model is created from these results.

Instead of clustering after an inversion to achieve the effect of a cooperative inversion like Paasche et al. (2006), Sun and Li (2015) use the FCM function as an extra term in the model objective function. This allows them to simultaneously invert slowness and density (from travel time and gravity data) by linking them

through the FCM clusters. It also allows them to guide the FCM cluster physical properties in a way that allows the integration of petrophysical measurements of geological units without directly forcing where the units are in space.

Finally, I will discuss implementations of constrained inversions. Phillips (2001) uses bore hole densities and susceptibilities to bound a gravity and a magnetic inversion. Farquharson et al. (2008) use density bore hole logs to create a reference model for a gravity inversion. They demonstrate the effect of having many bore holes versus only a few. Williams (2008) provides the most extensive review of this subject. He creates a software package to integrate a phenomenal number of types of geological and petrophysical data. Many of the tools that he created are integrated into the work that I present. He then uses these tools to make detailed susceptibility and density constraints. Finally, Lelievre (2009) discusses the use of surface samples and bore holes in constraining a synthetic example. He also shows the use of orientation information of linear features as a geological constraint.

As stated in the research motivation, what is lacking in previous implementations is an integrated environment where data, models, inversions, and constraints can be developed. By implementing the creation of constraints in such an environment, I make the creation of constraints faster even in non-trivial contexts with multiple sources of information and multiple forms of constraints.

1.4 Thesis Organization

In this thesis I describe the methods used to create the tools I contributed to GIFtools and give examples of their use. Chapter 2 will discuss the tools I have created. It describes the types of information that GIFtools and Model Builder can integrate into an inversion and discuss how they can be used to constrain an inversion result. I discuss how sample information (bore hole and surface sample data) can be used to set reference models and bounds. I also discuss geological maps and how Model Builder incorporates information from both cross section and plan view maps into the regularization of inversions. I also discuss parametric style inversions using a standard mesh and forward operator. Instead of allowing all cells to vary freely I constrain them to some number of units that must all be constant across the unit. Finally in Chapter 2 I discuss the use of clustering multiple inversion results to

create non-trivial face weights in addition to reference models and bounds.

In ?? I show the use of GIFtools and Model Builder in the creation of regularizations for a magnetic inversion in El Poma. El Poma is a porphyry deposit in Colombia that has magnetic properties measured from bore holes, surface samples, in addition to a geological map over the region. The region is also interesting due to the large effect of remanent magnetization. I discuss a synthetic case matching the magnetic survey, bore holes, surface samples and map to recover the anomaly. I also show the result of the inversion of the actual field data.

Finally in Chapter 3 I show an example GIFtools and Model Builder in the context of the Tli Kwi Cho Kimberlite complex in the North West territories. In this case there have been several surveys flown over the region for electromagnetic (of which I use only the magnetic data) and gravity gradiometry data. In addition to the geophysical data there has been extensive drilling and cross section maps have been created. I show a synthetic example inverting both gravity gradiometry and magnetic data incorporating the *a priori* information as well as using clustering of the magnetic and gravity inversion results to create further constraints.

Chapter 2

Tools for Integrating Geological and Petrophysical Information into Regularization

2.1 Including Sample Information (Bore Hole and Surface Sample) in Inversion Regularization

Bore holes provide physical property measurements at depth either by sending geophysical instruments down hole or by recovering a core and then measuring it subsequently in the lab. Much work has been done on including physical property bore hole information(Williams (2008)). In this section I discuss the way GIFtools and Model Builder incorporate bore hole information into inversion constraints.

In addition to physical property data, bore holes can also provide qualitative rock unit information. In this section I show the conversion of lithology information from bore holes into physical property information (using petrophysical measurements of reasonably similar rocks). Once this conversion is done, the bore hole information can be used in the same fashion as a physical property bore hole logs.

In this section I also show the advantage to integrating the creation of inversion constraints with more general data processing tools. Once we have a set of sample

data either bore hole or surface sample loaded into GIFtools we can then use the general data modification tools that are already provided for data quality control.

2.1.1 Importing Bore Hole Data

Bore hole data is typically stored in three separate files: the collar file, the survey file, and the property file. I now discuss the information contained in each file. The collar file contains the spacial information of the very top of the hole often called the collar. Table 2.1 shows an example collar file. GIFtools is sufficiently flexible that it can read both whitespace and comma delimited files, additionally as long as there are headers for each column, it does not matter what order the columns appear in, as the correct columns for each purpose can be specified during the import process, finally while the example shows a text hole identifier, it is also possible to identify individual hole by a numerical index.

| ! comment | | | | | |
|------------|--------|---------|-----|--------|--|
| HOLE-ID | X | Y | Z | LENGTH | |
| DO27-05-01 | 557187 | 7133758 | 418 | 58.52 | |
| DO27-05-02 | 557191 | 7133755 | 418 | 459.5 | |
| DO27-05-03 | 557165 | 7133682 | 418 | 230 | |
| DO27-05-04 | 557425 | 7133835 | 420 | 112.5 | |
| DO27-05-05 | 557425 | 7133835 | 420 | 99.8 | |
| DO27-05-06 | 557425 | 7133835 | 420 | 101 | |
| DO27-05-07 | 557425 | 7133835 | 420 | 218 | |
| DO27-05-08 | 557392 | 7133834 | 419 | 290 | |
| DO27-05-09 | 557392 | 7133834 | 419 | 155 | |
| DO27-05-10 | 557392 | 7133834 | 419 | 140 | |
| DO27-05-11 | 557400 | 7133913 | 419 | 374 | |
| DO27-05-12 | 557345 | 7134210 | 419 | 65 | |

Table 2.1: An example collar file from TKC bore holes

The survey file provides depth, azimuth, and dip information, coding how the hole changes direction below the collar. In Table 2.2 all the holes as defined in Table 2.1 are straight and dip in different directions.

Finally, the property file contains information about a given property down the hole. This property can either be a physical property (e.g. density, susceptibility,

| ! | comment | | | |
|---|------------|-------|---------|-----|
| | HID | DEPTH | AZIMUTH | DIP |
| | DO27-05-01 | 58.52 | 0 | -90 |
| | DO27-05-02 | 0 | 0 | -90 |
| | DO27-05-02 | 459.5 | 0 | -90 |
| | DO27-05-03 | 0. | 0 | -90 |
| | DO27-05-03 | 230 | 0 | -90 |
| | DO27-05-04 | 0 | 180 | -70 |
| | DO27-05-04 | 112.5 | 180 | -70 |
| | DO27-05-05 | 0 | 200 | -47 |
| | DO27-05-05 | 99.8 | 200 | -47 |
| | DO27-05-06 | 0 | 80 | -45 |
| | DO27-05-06 | 101 | 80 | -45 |
| | DO27-05-07 | 0 | 273 | -70 |
| | DO27-05-07 | 218 | 273 | -70 |
| | DO27-05-08 | 0 | 265 | -45 |
| | DO27-05-08 | 290 | 265 | -45 |
| | DO27-05-09 | 0 | 265 | -86 |
| | DO27-05-09 | 155 | 265 | -86 |
| | DO27-05-10 | 0 | 348 | -45 |
| | DO27-05-10 | 140 | 348 | -45 |
| | DO27-05-11 | 0 | 240 | -45 |
| | DO27-05-11 | 374 | 240 | -45 |
| | DO27-05-12 | 0 | 230 | -45 |
| | DO27-05-12 | 65 | 230 | -45 |

Table 2.2: An example survey file from TKC bore holes (same holes as Table 2.1

etc.) or a geological unit. The depth information of a property measurement can be stored as a simple depth along the bore hole, or as an interval with two depths a “from” and a “to” depth stating that a given measurement hold for the whole interval. Table 2.3 shows the second form of property file with a numerical lithology.

The process to load bore hole data into GIFtools is as follows. Firstly the files that define the bore hole data set (collar, survey, and property) need to be provided. Secondly, the columns to be imported from the property file need to be stated. Lastly the method by which the property data is linked spatially to the drilling

| ! | comment | | | |
|------------|---------|-------|-------|--|
| HOLE-ID | FROM | TO | LITHO | |
| DO27-05-01 | 56.5 | 58.52 | 1 | |
| DO27-05-02 | 56 | 459.5 | 1 | |
| DO27-05-03 | 59 | 230 | 1 | |
| DO27-05-04 | 19 | 63.4 | 1 | |
| DO27-05-04 | 63.4 | 112.5 | 3 | |
| DO27-05-05 | 21.8 | 85.8 | 1 | |
| DO27-05-06 | 37 | 49.5 | 1 | |
| DO27-05-06 | 49.5 | 82.9 | 3 | |
| DO27-05-07 | 20.5 | 104.5 | 1 | |
| DO27-05-07 | 104.5 | 131 | 3 | |
| DO27-05-07 | 138.7 | 218 | 2 | |
| DO27-05-08 | 20.8 | 290 | 1 | |
| DO27-05-09 | 9 | 95.8 | 1 | |
| DO27-05-09 | 95.8 | 117 | 3 | |
| DO27-05-09 | 125.4 | 155 | 2 | |
| DO27-05-10 | 17 | 100.3 | 1 | |
| DO27-05-10 | 100.3 | 123 | 3 | |
| DO27-05-11 | 44.5 | 223.5 | 1 | |
| DO27-05-12 | 36 | 36.7 | 2 | |

Table 2.3: An example survey file from TKC bore holes (same holes as Table 2.1)

data (collar and survey) is stated. All of these are done by the GUI as shown in Figure 2.1. Note that the user has to set whether the depth information of the property

There are two methods to link property and drilling data, discrete and interpolation. If the discrete option is selected then GIFtools simply determined the spatial location based on the depth provided in the property file. In the case that the depth is given in the form of intervals, the depth of the measurement is considered to be the midpoint of the interval.

If interpolate is selected the program behaves differently depending on whether the depth information is simple depths or intervals. In both cases instead of using the depth information directly, a sample is provided at each point along the bore hole with distances between each sample defined by the sampling interval value in

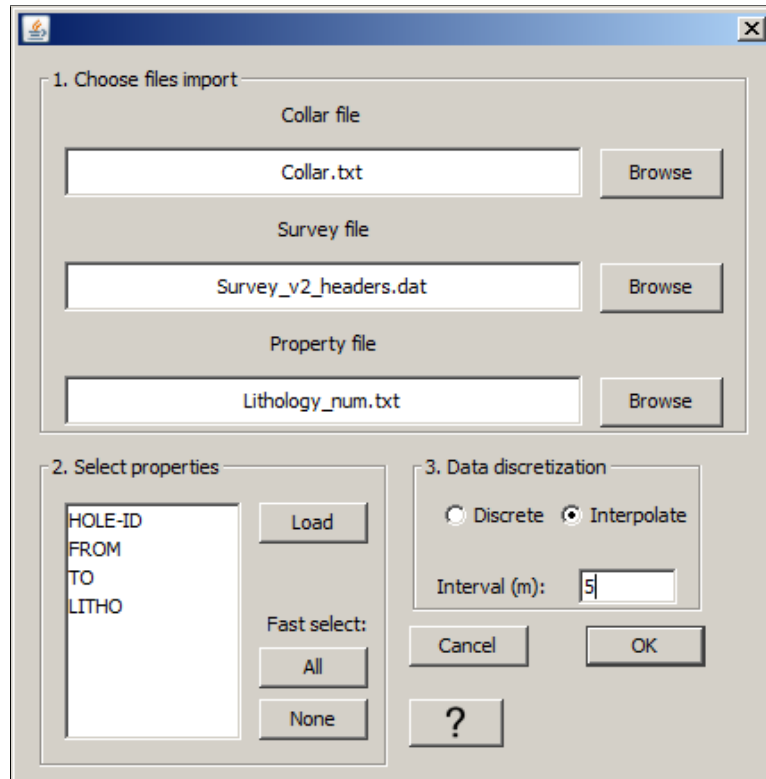


Figure 2.1: The first GUI for importing bore hole data

the first GUI (Figure 2.1).

In the case of simple depths, it is assumed that the measurement is some physical property, and given the sample depths the measurements are linearly interpolated along the bore hole. In the case of intervals it is assumed that the measurement lithologies which should not be interpolated, so samples with depths that are within an interval are assigned the property given while depths outside of any range are assigned a NaN value.

Once the files, and property location options have been set, the next step to importing bore hole data into GIFtools is the set of data columns and data headers. Since different collar, survey, and property files have different column orders it advantageous to allow the flexibility to assign columns with a given header to any property of the bore hole object in GIFtools. The GUI to assign the columns is

shown in Figure 2.2

Specify file headers for import

Collar file

Easting: X

Northing: Y

Elevation: Z

Hole ID: HOLE-ID

Hole length: LENGTH

Property file

Hole ID: HOLE-ID

Property: LITHO

☒ Intervals ☐ Depth

Depth: HOLE-ID

Interval from: FROM

Interval to: TO

Survey file

Depth: DEPTH

Azimuth: AZIMUTH

Dip: DIP

Hole ID: HID

Cancel OK

?

Figure 2.2: The second GUI for importing bore hole data

2.1.2 Visualizing Bore Hole Data

As stated in the introduction to this section, one of the advantages of integrating the Model Builder tools (including these tools for bore hole data being described) into GIFtools, a more general data visualization and quality control environment, is the ability to use those same tools for the data with which we create regularizations. In this case it is very useful to be able to visualize bore hole data before it gets incorporated in reference model and bounds of an inversion.

Figure 2.3 show the visualization of the bore hole data from TKC, note that the data has been sampled within each unit. Figure 2.4 show the visualization of a physical property bore hole data set from El Poma. Note that instead of the blocky sampling each datum along the hole was given its own position (the mid point of each small interval). In both cases the value of the visualized property of a given hole is shown along the side of the 3D representation of all the holes.

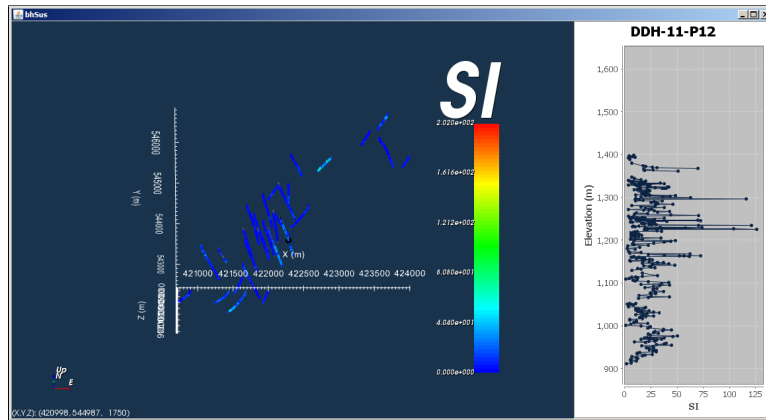


Figure 2.3: Visualization of TKC lithology bore hole data

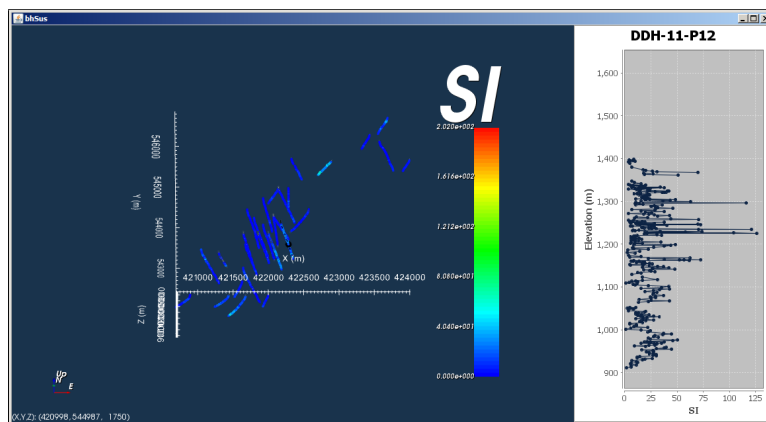


Figure 2.4: Visualization of El Poma susceptibility bore hole data

2.1.3 Converting Lithology Information into Petrophysical Information

2.1.4 Discretizing Bore Hole Data

- Provide mesh, Usually from Model Builder
- describe distribution
 - normal
 - log normal

- describe why one and not other. Cond tends to be log normal (citation needed), Den tends to be normal (citation needed), Susc can be either depending on who you ask(citation needed).
- describe method of determining bounds
 - Confidence interval: given a number of samples in a cell and a distribution, bounds are determined from a given percent confidence interval. Where the standard deviation is zero, (if there is only one datum, or all the data are equal) the minimum value is used in place of the confidence interval.
 - Floor: Simply assigns a bound based on the mean value of each cell plus or minus the provided floor value
 - Standard Deviation: Calculates the standard deviation of the sample values in each mesh cell (given a normal or log normal distribution). The bounds are set as equal to the mean value plus some multiple of the standard deviation. In the case that the standard deviation is zero the minimum value is used instead of the multiplied standard deviation.
- positivity simply set the lower bound and mean to be at least 0

2.1.5 Editing Bore Hole Data

- show editing of BH discretization
- show editing of prop data for susc to eff susc

2.1.6 Making Constraint

- show resolve conflicts dialogue
 - steal from below section (new images necessary)

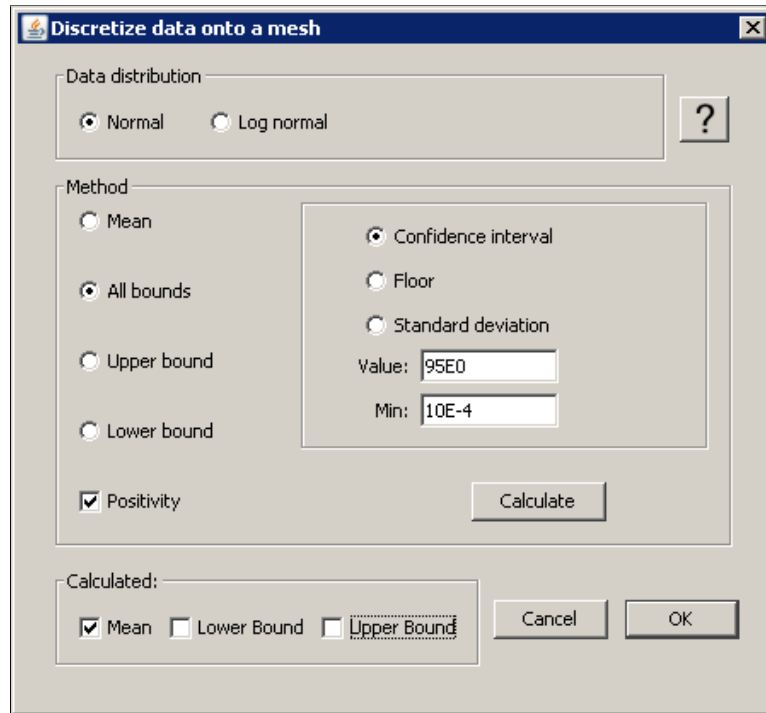


Figure 2.5: GUI to allow the discretization of bore hole data to a given mesh

2.1.7 Surface Sample

In addition to physical property measurements down hole, physical properties can also be measured on the surface, in many cases with much more ease. As with bore hole data, much work has been done on including surface sample information in inversion regularization. Surface Samples take on increased importance since in general the sensitivity of the data on a given cell is higher when the cell is nearer the surface. Constraining these surface cells can reduce artifacts that come from this increased sensitivity.

- show loading, visualization, editing, all similar to BH

2.2 Including Geological Maps in Inversion Regularization

It is often the case that geological information is provided in the form of geological maps in either cross section or plan view. Such maps are particularly useful since they provide a great deal of information over their entire surface. Cross sections can provide information at depth and constrain a whole region often within the center of a target of interest. Plan view maps do not provide information at depth, but they do constrain the entire surface of the region being inverted. Constraining the surface of an inversion is of interest since the sensitivity of the data to the top cells is particularly high, which can lead to artifacts on the surface. For the next section the plan view model is from the El Poma case study and the cross section model is from TKC, specifically the map from (Harder et al., 2006)

Below in point form is the method I have developed to incorporate pixel maps.

2.2.1 Preprocessing images

Often a geological map image will not be immediately suitable to the methods used below and some preprocessing is required. The most notable features that are undesirable in a map are geological units that are not only one or two colours and text or other annotations that could be interpreted by the program as geological information. Also map images may be of too high resolution to be efficiently used in these methods and must also be down-sampled to save computer processing time and memory.

For example Figure 2.6 has great deal of information, (faults, magnetic susceptibility surface samples, etc.) that are not information about geological units. In addition the geological units are not a single colour polygon. The image has been edited in the GNU Image Manipulation Program (GIMP), a free image editing program, to produce Figure 2.7.

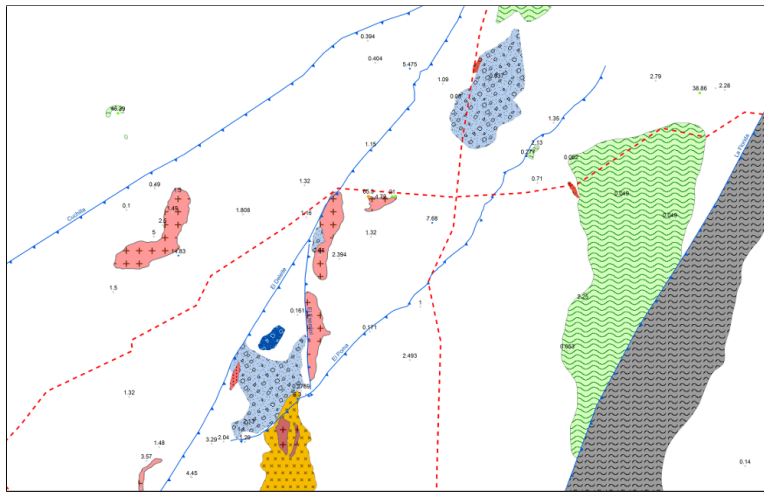


Figure 2.6: The El Poma map with fault lines (blue lines with barbs) included

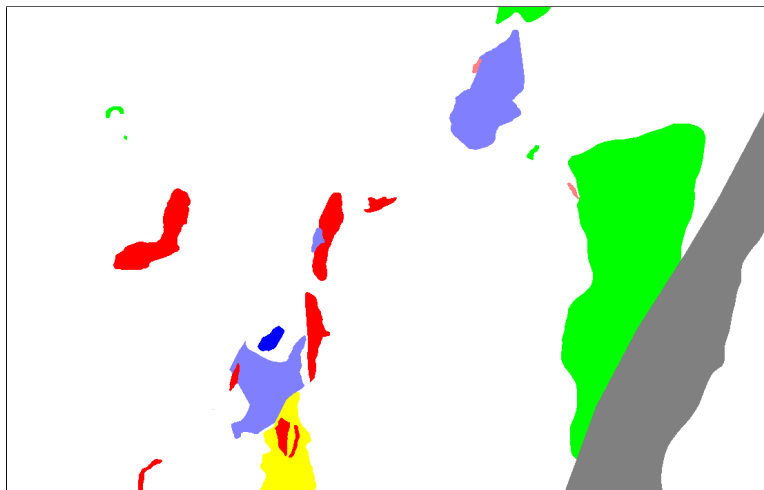


Figure 2.7: The El Poma map with extra information removed and geological units made a single colour

2.2.2 Loading Images into GIFtools

- load image into the GIFtools format (Figure 2.8)
 - Determine image format.
 - Load image using MATLAB utilities.

- Convert image into .png style representation for faster computation.
 - Using .twf file (world file) assign location and spacial resolution to the image.
 - Assign a legend linking pixel RGB values to geological unit.
 - Assign topography (either number or GIFtools TOPOdata item) for visualization.
- * In the case of a cross section image, instead of topography, information for the location of the cross section in 3D or 2D space is required (Figure 2.9).

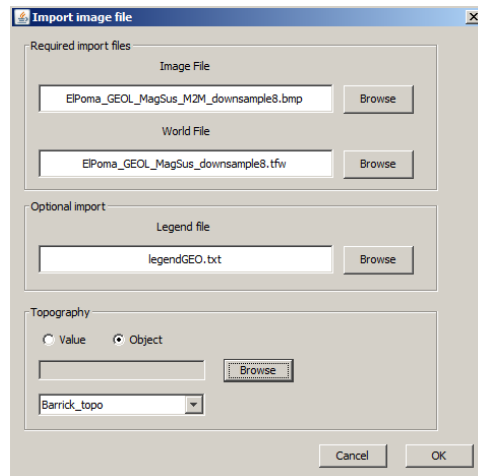


Figure 2.8: GUI for importing plan view image

Storing a map as a GIFtools object allows its use in several ways. Notably it allows the integration of the map with models and data, allowing figures overlaying the map and data or model and allowing interpretation of the data or model with direct reference to the map (Figure 2.10).

2.2.3 Creating a Pixel Map Legend

Continuing on in the process of making a geological constraint.

- Find the geological unit represented of each pixel.

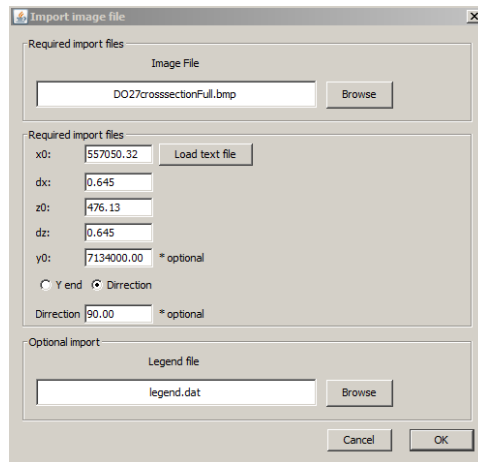


Figure 2.9: GUI for importing cross section image

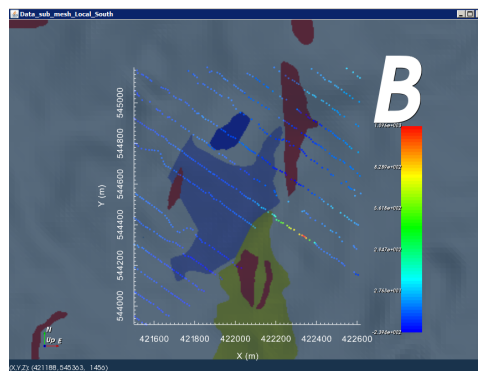


Figure 2.10: Example of magnetics data being viewed with a map overlaid

- In the .png style format as stored in MATLAB, an image consists of an “image” field, a matrix of integers, and a “map” field, which maps the image matrix to RGB value triplets.
- Each RGB triplet is compared to the legend that was provided when the image was loaded. A map field entry is considered to represent a geological unit if all three components of the RGB triplet are within a provided tolerance of any entry in the legend.
- Now that we have a relation of entries in the map field to geological units in the legend, we can assign a geological unit to each pixel in

the original image simply by applying the new geological map to the image field.

2.2.4 Making a Geology Model from Map

Plan View

- Provide active model. For convenience this is usually an active model already associated with a Model Builder object.
 - The active model simultaneously provides a discretized topography for the map to lay along and also a mesh (GIF 3D tensor or OcTree).
- Provide some form of depth information.
 - Thickness, a certain amount of depth below topography at each point will be assigned the geological unit at each.
 - Depth, the map will be used to assign a geological unit down to a fixed depth across the whole model.
 - Surface, if you provide another surface below topography the cells between topography and the other surface will be assigned.
- Crop all pixels that extend outside of the mesh or that represent the background geological unit.
 - The cropping greatly speeds up the process and makes it require much less computer memory.
 - Furthermore, in the event of a mistake with coordinates the process ends almost instantly as there are few pixels to process.
- Finally the geological model is created.
 - We determine which cell of the mesh each pixel is in, including those cells below each pixel to account for thickness.
 - Each cell is assigned a geological unit based on the mode of the geological values of each pixel which colours that cell. In other words,

each cell is identified with the geological unit which fills the greatest proportion of the cell.

- * The mode is used since each cell will be a particular unit. Since the property being mapped onto each cell by construction must represent a single geological unit, interpolation between the units will not provide the desired result.
- The geology definition which will allow the assignment of physical properties to each geological unit. The result is shown in Figure 2.11, the continuous colour bar is not an indication of a continuous model. All model values are integers that represent geological units in the map.

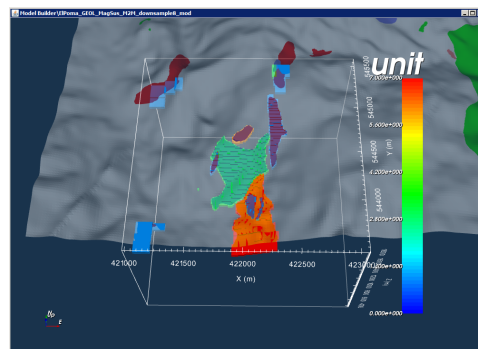


Figure 2.11: Example of a geology model created from a map with the map overlaid

Cross Section

The cross section case follows much the same procedure with a few exceptions. An imported cross section map is shown overlaid on a 2D mesh in Figure 2.12. Notably no parameter for the vertical extent is needed. The other notable exception is that mesh that is used is a GIF 2D mesh. The result is shown in Figure 2.13.

A 2D Geology model can be used to create constraints for a 2D inversion, it can also be used to add constraints to a 3D inversion as well. After the 2D geology model is created from the cross section map, it can be inserted into a 3D mesh (GIF 3D tensor or OcTree) given a starting and ending position or a starting position and

a direction Figure 2.14, Figure 2.15.

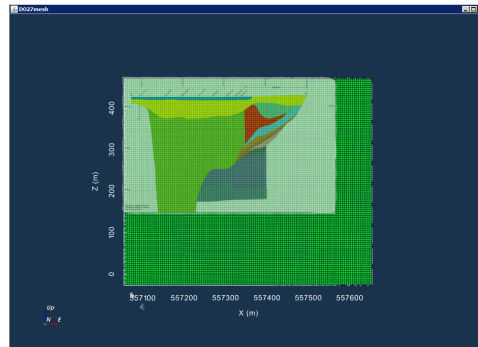


Figure 2.12: Example of a 2D mesh with the map overlaid

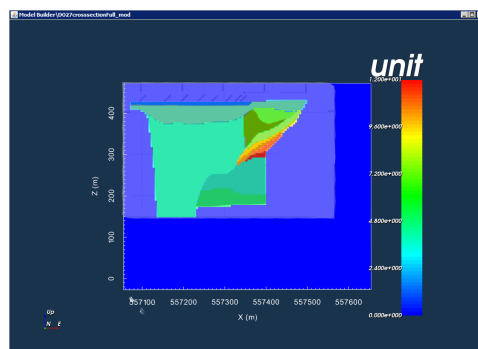


Figure 2.13: Example of a 2D geology model created from a cross section map with the map overlaid

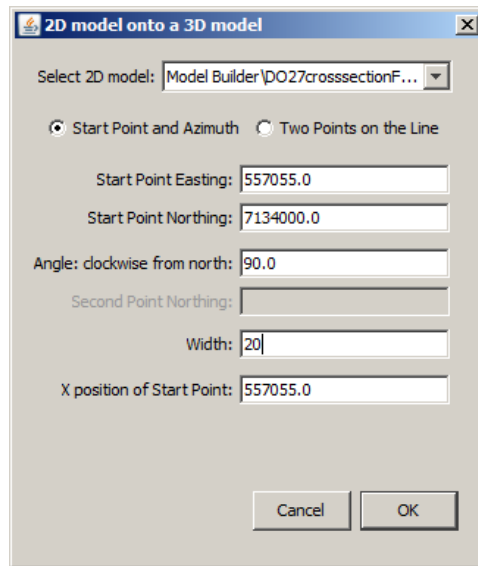


Figure 2.14: GUI for adding a 2D model to a 3D model

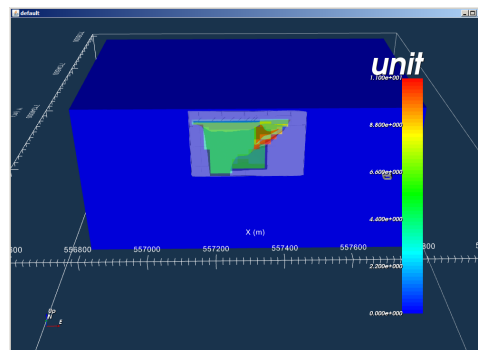


Figure 2.15: Example of a 2D geology inserted into a 3D model with the map overlaid

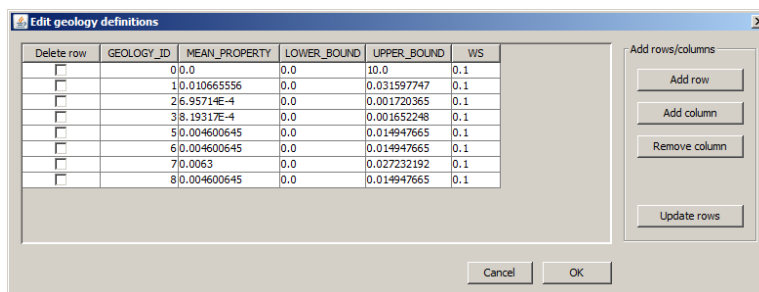
2.2.5 Making Constraints for an Inversion

The model that has been created is a geology model. That is, a model in which each cell represents a given geological unit. To be able to convert this model into a constraint for a geophysical inversion the link between between the geology and the petrophysics needs to be provided.

The link is stored in what is called a geology definition. In GIFtools this takes

the form of a lookup table that contains information of each particular geological unit's property, lower and upper bounds, and optionally the smallness weight associated with each unit.

Using the geology definition we can convert a geology model that has information about the spatial distribution of geological units but not of their physical properties into constraints that are usable by an inversion. In the figures below the geological definition came from surface measurements of magnetic susceptibility within each geological unit. Figure 2.16 is an example of a geology definition in the GIFtools GUI.



| Delete row | GEOLOGY_ID | MEAN_PROPERTY | LOWER_BOUND | UPPER_BOUND | WIS |
|--------------------------|------------|---------------|-------------|-------------|-----|
| <input type="checkbox"/> | 0 | 0.0 | 0.0 | 10.0 | 0.1 |
| <input type="checkbox"/> | 1 | 0.010665556 | 0.0 | 0.031597747 | 0.1 |
| <input type="checkbox"/> | 2 | 6.95714E-4 | 0.0 | 0.001720365 | 0.1 |
| <input type="checkbox"/> | 3 | 8.19317E-4 | 0.0 | 0.001652248 | 0.1 |
| <input type="checkbox"/> | 5 | 0.004600645 | 0.0 | 0.014947665 | 0.1 |
| <input type="checkbox"/> | 6 | 0.004600645 | 0.0 | 0.014947665 | 0.1 |
| <input type="checkbox"/> | 7 | 0.0063 | 0.0 | 0.027232192 | 0.1 |
| <input type="checkbox"/> | 8 | 0.004600645 | 0.0 | 0.014947665 | 0.1 |

Figure 2.16: Example of a geological definition as displayed in the GIFtools GUI

Once the geology definition is provided, we can use the Combine Model Dialog (Figure 2.17) in Model Builder to create a reference model and bounds. In this case the resolution of conflicts is trivial as there is a single source of information. Less trivial examples of the creation of reference models and bounds will be discussed later. The resulting reference model is shown in Figure 2.18.

2.2.6 Inputing Fault information from Geological Maps

Another piece of information that can be in geological maps are fault locations. Again in the context of El Poma the map provided a whole complex of thrust faults as shown in the un-doctored map in Figure 2.6

The method used to insert faults into an inversion is as follows:

- Determine the end points of the fault.

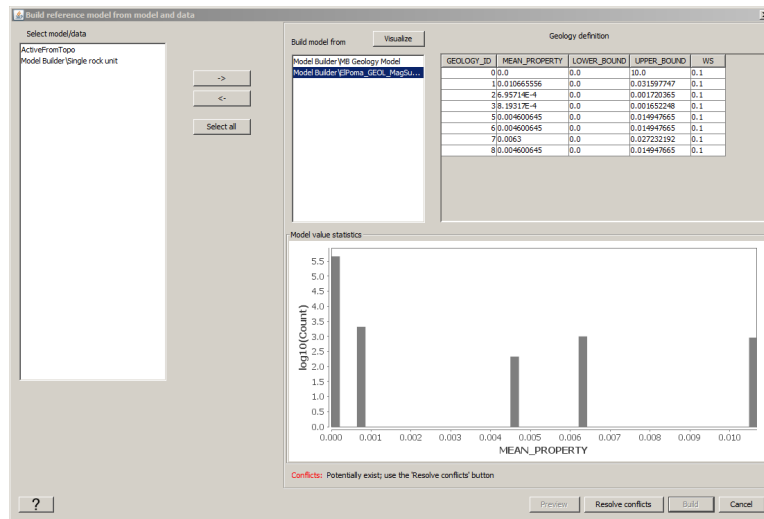


Figure 2.17: Example of a typical combine model dialog for a reference model

- GIFtools makes this easy by reporting the location of the cursor in the data viewer allowing you to find the location (including elevation) of a point along the fault.
- Using the locations provided GIFtools creates the fault weights by creating a two boxes, each with one of its sides along the fault location as defined in the GUI. By setting the value of cells in each box to one, and then taken the derivative of each model, two face models are created where only faces along the fault as defined are non-zeros. Finally by searching for non-zero elements and finding the intersect between the two models, it is possible to set the values of the the faces that define the fault to any value desired.
- faces within this box are assigned a new value that is provided in the GUI Figure 2.19.

This process can be done multiple times to create non-trivial fault complexes as shown in Figure 2.20

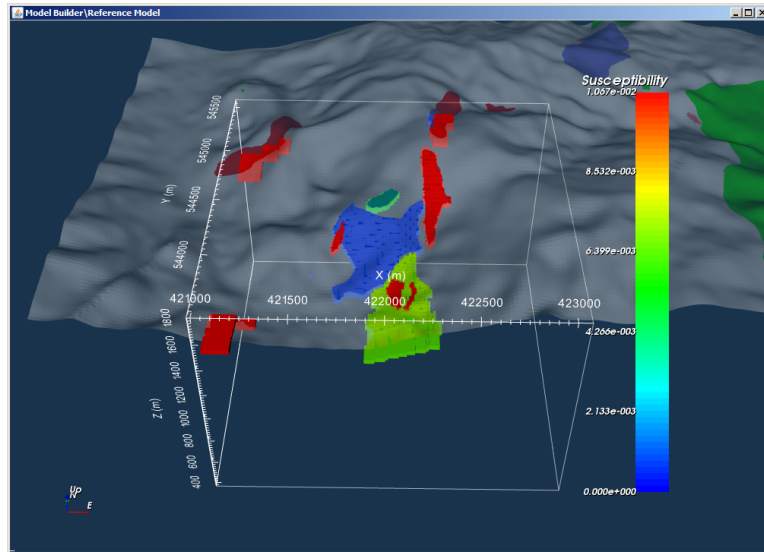


Figure 2.18: Example of a reference model created from a geological map

| Spatial Information | |
|---------------------|------------------|
| First Point | First Point |
| Easting: 421938 | Easting: 423863 |
| Northing: 544163 | Northing: 595063 |
| Elevation: 1380 | Elevation: 1661 |

| Other Information | |
|-------------------|--------------------------|
| Dip: 30 | Which Weights to Assign? |
| Width: 7.5 | |
| Fault Value: 1E-2 | |

| |
|---|
| <input checked="" type="checkbox"/> x weights |
| <input checked="" type="checkbox"/> y weights |
| <input checked="" type="checkbox"/> z weights |

Cancel OK

Figure 2.19: The GUI for the creation of fault weights

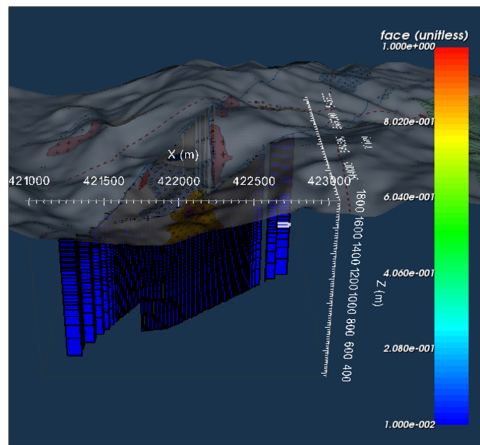


Figure 2.20: An example of fault weights that can be created with GIFtools

2.3 Clustering to Create Pseudo-geologic Constraints

2.3.1 Clustering Algorithms

In contexts where multiple data types have been collected over an area, it is often of interest to include information from one inversion result in the regularization of another. Much work has been done on this topic (see Section 1.3).

One possible way of integrating information from another inversion result is through clustering to create pseudo-geological models, and then using these to create reference models, bounds, and smoothness weights to constrain subsequent inversions.

Given several inversion of different data types, multiple models of different physical properties can be recovered. Assuming that each recovered model is on the same mesh (either because all inversion were performed on the same mesh or the were interpolated onto the same mesh after the fact) each cell has a value for each physical property. Since the standard representation of a model is a vector $\mathbf{m} \in \mathbb{R}^M$ where as in Equation 1.2 M is the number of cells in the discretization of the earth model, we can generalize so that $\mathbf{M} \in \mathbb{R}^{M \times l}$ is the compiled results of l inversion. This notation allows us to say that \mathbf{M} is made out of several m_i for $i = 1 \cdots l$ and where each m_i is a row vector l long.

In each case the algorithm depends on the user providing the number of clusters for analysis. The Clustering method used determines the clusters and the membership of each m_i in the clusters.

The first clustering methods implemented in Model Builder is simply user defined boundries. These allow a great deal of user control and can be very useful assuming something is known about the underground geology or the physical properties of given units. On the other hand it can quickly be untenable to use this method if several clusters are need or many recovered models are being clustered.

The second clustering method implemented in Model Builder is k-means clustering GAF (1984) which is based on the minimization of the following objective function,

$$\phi_{k-mean} = \sum_{j=1}^k \sum_{m_i \in S_j} \|m_i - v_j\|_2^2, \quad (2.1)$$

where k is the number of clusters and S_j are the sets of model cells m_i that make up the clustering, finally v_j are the centroids of each cluster. The algorithm to minimize ϕ_{k-mean} is a two step process firstly assigning each m_i to a cluster S_j and secondly determining a new set of v_j that better fit the data.

Finally, the third clustering algorithm implemented in Model Builder is Fuzzy C-Means (FCM) (Sun and Li, 2015). FCM is a generalization of Equation 2.3.1 where instead of each datum m_i being in only one cluster, each datum is assigned membership in each cluster to varying degrees allowing “fuzziness” in the classification. The objective function becomes

$$\phi_{FCM} = \sum_{j=1}^k \sum_{i=1}^M u_{ij}^q \|m_i - v_j\|_2^2, \quad (2.2)$$

where instead of the k sets S_j , membership in each cluster is represented by the membership matrix $u \in \mathbb{R}^{M \times k}$. Each row of u must sum to 1, in other words each datum is fully considered in u but may be classified as partially in each cluster. Finally q , controls the “fuzziness” of the clustering with a value of $q = 1$ making a non-fuzzy clustering with each datum being in only one cluster and amount that a given datum can be in multiple clusters increasing as the value of q increases.

In the case of the clustering algorithm used in Model Builder the final step is “de-fuzzification”, that is the determining of the cluster that each model cell most fits in. Each model cell is assigned the cluster for which it has the highest membership value.

In both the k-means and the FCM case the minimization of the objective functions is done by the standard MATLAB function and notably the value of q in the FCM case is set at 2.

2.3.2 Clustering In GIFtools and Model Builder

- describe requirements

- show GUI
- show result

2.3.3 Creation of Constraints

- show creation of ref and bounds from mean cluster boundaries
- show creation of sharp bounds with weights.

2.4 Voxel-Parametric Inversion to Provide Physical Property Values for Geological Models

In Section 2.3 geological models that span the whole discretized volume are defined. These are more extensive than the geological models described in Section 2.2.4 because each cell is classified into a cluster as opposed to most cells not having any information (due to the map not intersecting the cell at all in the case of most cells).

In addition to pseudo-geological models created by clustering, it is also possible to get geological models from drill or surface geological data. In TKC one of the forms of geological data that was provided was a set of points created from the interpreted interfaces between units determined using the lithological bore hole data shown in Figure 2.3. The point cloud of the interfaces is shown in Figure 2.21 and the resultant geological model created using the add non-convex polyhedron command is shown in Figure 2.22.

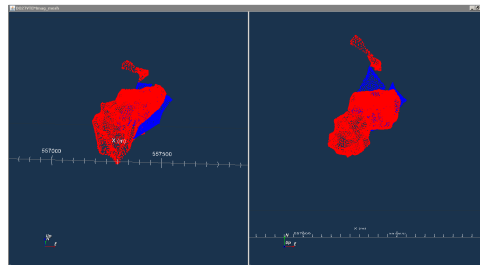


Figure 2.21: Point cloud of the geological interfaces for TKC bore hole data

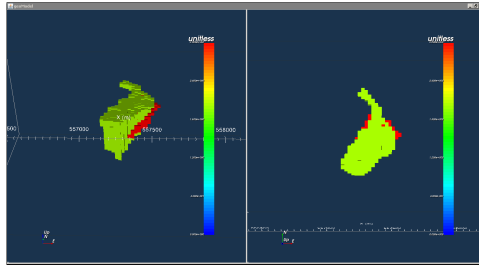


Figure 2.22: A geological model created from the data shown in Figure 2.21

In the cases listed above we have acquired a distribution of geological units that extend across the whole discretized volume it becomes interesting to go further into the assignment of physical properties to the geological units in question. In the case of a clustered pseudo-geological model the obvious method of property assignment is simply using the centroid value recovered from the clustering algorithm. In addition a standard deviation from the mean can be acquired to set the upper and lower bounds of each unit.

Another option is the direct assignment of measured physical property values to the (pseudo-)geological units. This method has the advantage of directly incorporating physical property data into the inversion constraints. Direct assignment can be done through the GIFtools GUI by editing the geologic definition of the geological model, and this method makes most sense when the model in question either is the products of geological modeling as in Figure 2.22 or there is a strong parallel between the clustered units and actual geological units.

In some cases the above method leaves something to be desired. In the case of cluster centroids, artifacts in the inversion can lead to magnitudes in the recovered model not being quite in scale with the physical properties in the ground, additionally this method only works if the geological model in question was derived through clustering. In the case of the direct assignment of measured physical properties to geological units, the properties often vary a great deal across the earth model. This can be due to large scale variation across the geological unit (such as be alteration) or small scale alteration where one portion of a sample can be significantly more susceptible than another.

2.4.1 Formulation of Voxel-Parametric inversion problem

As stated in Section 1.2 and Equation 1.2, the forward problem for which we are trying to find the inverse is formulated as follows

$$\mathbf{d} = \mathbb{F}[\mathbf{m}], \quad (2.3)$$

where as stated above $\mathbf{d} \in \mathbb{R}^N$ is the geophysical data, $\mathbf{m} \in \mathbb{R}^M$ is a discretization of m which is the model that describes the distribution of some physical property, and \mathbb{F} is the forward operator that mediates between them. \mathbb{F} can be considered to be a matrix of size $N \times M$ which in the case of a non-linear problem has a dependence on the model m but in the case of linear problem (such as potential field problems) there is no such dependence. With this in mind Equation 2.4.1 can be re-written

$$\mathbf{d} = \mathbb{F}(\mathbf{m})\mathbf{m}, \quad (2.4)$$

- show that geological model can collapse the forward operator to much smaller matrix by assuming that each unit has a single property value.
 - especially when the background is fixed at zeros and has no sensitivity
- describe optimization of new parametric inversion with many fewer degrees of freedom
- describe uses of the new model
 - assign properties to geological models that fit the collected data as closely as possible
 - * perhaps allows the geology constraints as in Section 2.3.3 to be more accurate
 - * allows the determination of magnetization direction given a geologic or pseudo-geologic model of an magnetization anomaly

- * allows the creation of synthetic models that roughly fit data that has already been acquired

2.5 Conclusion

In this section I have shown the creation of constraints that are compatible with GIF inversion codes. I have created these constraints from multiple types of map (Cross Section and Plan View) and have used different pieces of information from these maps (geological units and fault locations).

Chapter 3

Case Study #2 TKC

3.1 Overview of Deposits

3.2 Discussion of the Geophysical Data Given

3.3 What Information is Available

3.4 Synthetic Model

3.5 Blind Inversion of the Synthetic Model

3.6 Determination of Magnetization Direction

3.7 Creation of Constraints and Types of Data

3.7.1 α coefficients

3.7.2 Reference Models

3.7.3 Weighting matrices

3.7.4 Bounds

Bibliography

- Barbosa, V. C., and J. B. Silva, 2006, Interactive 2d magnetic inversion: A tool for aiding forward modeling and testing geologic hypotheses: *Geophysics*, **71**, L43–L50. → pages 7
- Barbosa, V. C. F., and J. B. Silva, 1994, Generalized compact gravity inversion: *Geophysics*, **59**, 57–68. → pages 7
- Bosch, M., A. Guillen, and P. Ledru, 2001, Lithologic tomography: An application to geophysical data from the cadomian belt of northern brittany, france: *Tectonophysics*, **331**, 197–227. → pages 7
- Chasseriau, P., and M. Chouteau, 2003, 3d gravity inversion using a model of parameter covariance: *Journal of applied geophysics*, **52**, 59–74. → pages 7
- Farquharson, C. G., M. R. Ash, and H. G. Miller, 2008, Geologically constrained gravity inversion for the voisey’s bay ovoid deposit: *The Leading Edge*, **27**, 64–69. → pages 2, 8
- Farquharson, C. G., and D. W. Oldenburg, 1998, Non-linear inversion using general measures of data misfit and model structure: *Geophysical Journal International*, **134**, 213–227. → pages 6
- Fournier, D., 2015, A cooperative magnetic inversion method with lp-norm regularization: PhD thesis, University of British Columbia. → pages 6
- GAF, S., 1984, Multivariate observations. → pages 31
- Guillen, A., P. Calcagno, G. Courrioux, A. Joly, and P. Ledru, 2008, Geological modelling from field data and geological knowledge: Part ii. modelling validation using gravity and magnetic data inversion: *Physics of the Earth and Planetary Interiors*, **171**, 158–169. → pages 7
- Guillen, A., and V. Menichetti, 1984, Gravity and magnetic inversion with minimization of a specific functional: *Geophysics*, **49**, 1354–1360. → pages 7
- Guitton, A., 2012, Blocky regularization schemes for full-waveform inversion: *Geophysical Prospecting*, **60**, 870–884. → pages 6
- Harder, M., C. Hetman, B. Scott Smith, and J. Pell, 2006, Geology of the do27 pipe: a pyroclastic kimberlite in the lac de gras province, nwt, canada: Presented at the Long abstracts, Kimberlite Emplacement Workshop,

- Saskatoon, Sask. Available at <http://www.venuewest.com/8IKC/files/14%20Harder.pdf> [accessed 18 June 2008]. → pages 19
- Last, B., and K. Kubik, 1983, Compact gravity inversion: *Geophysics*, **48**, 713–721. → pages 6, 7
- Lelièvre, P. G., 2009, Integrating geologic and geophysical data through advanced constrained inversion. → pages 2, 8
- Lelièvre, P. G., and D. W. Oldenburg, 2009, A comprehensive study of including structural orientation information in geophysical inversions: *Geophysical Journal International*, **178**, 623–637. → pages 7
- Li, Y., and D. W. Oldenburg, 1996, 3-d inversion of magnetic data: *Geophysics*, **61**, 394–408. → pages 2, 4, 5, 6
- , 1998, 3-d inversion of gravity data: *Geophysics*, **63**, 109–119. → pages 5, 6
- , 2000, Incorporating geological dip information into geophysical inversions: *Geophysics*, **65**, 148–157. → pages 6, 7
- , 2003, Fast inversion of large-scale magnetic data using wavelet transforms and a logarithmic barrier method: *Geophysical Journal International*, **152**, 251–265. → pages 5, 6
- Paasche, H., J. Tronicke, K. Holliger, A. G. Green, and H. Maurer, 2006, Integration of diverse physical-property models: Subsurface zonation and petrophysical parameter estimation based on fuzzy c-means cluster analyses: *Geophysics*, **71**, H33–H44. → pages 7
- Phillips, N. D., 2001, Geophysical inversion in an integrated exploration program: Examples from the san nicolas deposit. → pages 2, 8
- Portniaguine, O., and M. S. Zhdanov, 1999, Focusing geophysical inversion images: *Geophysics*, **64**, 874–887. → pages 6
- Rudin, L. I., S. Osher, and E. Fatemi, 1992, Nonlinear total variation based noise removal algorithms: *Physica D: Nonlinear Phenomena*, **60**, 259–268. → pages 6
- Sun, J., and Y. Li, 2015, Multidomain petrophysically constrained inversion and geology differentiation using guided fuzzy c-means clustering: *Geophysics*, **80**, ID1–ID18. → pages 7, 32
- Vogel, C. R., and M. E. Oman, 1998, Fast, robust total variation-based reconstruction of noisy, blurred images: *Image Processing, IEEE Transactions on*, **7**, 813–824. → pages 6
- Williams, N. C., 2008, Geologically-constrained ubc–gif gravity and magnetic inversions with examples from the agnew-wiluna greenstone belt, western australia. → pages 2, 8, 10

Appendix A

Supporting Materials

-